Tracer experiment and model evidence for macrofaunal shaping of microbial nitrogen functions along rocky shores

Catherine A. Pfister[1], Mark A. Altabet[2], Santhiska Pather[2], Greg Dwyer[1]

[1] Department of Ecology and Evolution, University of Chicago, Chicago IL, USA

[2] School for Marine Sciences and Technology, University of Massachusetts, Dartmouth, Bedford, MA, USA

Correspondence to: C. A. Pfister (cpfister@uchicago.edu)

Revised 16 May 2016 for Biogeosciences

Abstract. Seawater microbes as well as those associated with macrobiota are increasingly recognized as a key feature affecting nutrient cycling. Tidepools are ideal natural mesocosms to test macrofauna and microbe interactions, and we quantified rates of microbial nitrogen processing using tracer enrichment of ammonium ($^{15}N_{NH4}$) or nitrate ($^{15}N_{NO3}$) when tidepools were isolated from the ocean during low intertidal periods. Experiments were conducted during both day and night as well as in control tidepools and those from which mussels had been removed allowing us to determine the role of both mussels and daylight in microbial nitrogen processing. We paired time-series observations of ^{15}N enrichment in NH_4^+, NO_2^-, and NO_3^- with a differential equation model to quantify multiple, simultaneous nitrogen transformations. Mussel presence and daylight increased remineralization and photosynthetic nitrogen uptake. When we compared ammonium gain or loss that was attributed to any tidepool microbes versus photosynthetic uptake, microbes accounted for 32% of this ammonium flux on average. Microbial transformations averaged 61% of total nitrate use; thus, microbial activity was almost 3 times photosynthetic nitrate uptake. Because it accounted for processes that diluted our tracer, our differential equation model assigned higher rates of nitrogen processing compared to prior source-product models. Our in situ experiments showed that animals alone elevate microbial nitrogen transformations two orders of magnitude, suggesting that coastal macrobiota are key players in complex microbial nitrogen transformations.

Keywords: tide pools, enrichment experiment, *Mytilus californianus*, differential equation model, nitrification, nutrient fluxes

1. Introduction

Nitrogen cycle processes are carried out by a diversity of taxa, from microbes to macrofauna, that can all reside in the same habitat. Nevertheless, most studies tend to focus on characterizing and/or measuring the rate of only a single transformation at a time (e.g. nitrification or nitrate reduction), despite the co-occurrence of a diversity of nitrogen processes including those leading to loss or retention. Given an anthropogenic doubling over the past century of the supply rate of biologically available nitrogen to ecosystems (Galloway et al. 2008, Fowler et al. 2013) simultaneous with accelerated harvest of animals that recycle nitrogen (Worm et al. 2006, Maranger et al. 2008), it is essential that we understand how microbes and macrobiota interact to influence nitrogen cycling. Using the experimental tractability of rocky shore tidepools as natural mesocosms, coupled with isotope tracer enrichments and mathematical modeling, we estimate here the rate of simultaneous nitrogen transformations as a function of animal abundance and time of day.

Along upwelling shores, the paradigm of productivity driven by upwelled nitrate has been challenged by studies quantifying the effects of animal excretion and regeneration (Dugdale and Goering 1967, Aquilino et al. 2009, Pather et al. 2014). It is well known that nitrogen regeneration is quantitatively significant in a variety of ecosystems (Schindler et al. 2001, Vanni 2002, Allgeier et al. 2014, Subalusky et al. 2014), However, to make a significant contribution to productivity, uptake of animal excreted ammonium by photo- and chemolithotrophs needs to be sufficiently rapid to retain nitrogen locally to avoid dispersion into the larger environment.

Microbial nitrogen transformations are diverse, converting inorganic nitrogen among different biologically available (NH_4^+, NO_2^-, or NO_3^-) or unavailable (N_2) forms. Accordingly, the relative importance of these pathways also influences the retention or loss of regenerated nitrogen. In coastal environments, there is increasing documentation that microbial nitrogen transformation (e.g. chemolithotrophs) is intimately associated with animals (Welsh and Castadelli 2004, Pfister et al. 2010, Heisterkamp et al. 2013, Stief 2013). Rapid use of animal-regenerated ammonium is likely by both obligate ammonia oxidizing microbes (e.g. Ward 2008) as well as phototrophs that prefer it for energetic reasons (Magalhães et al. 2003, Zehr and Kudela 2011). Accordingly, ammonium production by animals may be an important contributor to the productivity along rocky shores of the northeast Pacific that are part of the California Current Large Marine Ecosystem (CCLME).

There is parallel evidence that marine animals host diverse microbiomes (Pfister et al. 2010, 2014b, Miranda et al. 2013, Moulton et al. 2016) as well as stimulate phototrophs with excreted nitrogen (Taylor and Rees 1998, Plaganyi and Branch 2000, Bracken 2004). Incubating seawater or sediment separate from the natural environment has provided controlled estimates of single nitrogen transformations (e.g. Yool et al. 2007). However, a principle challenge has been quantifying in situ the simultaneous nitrogen transformations that characterize natural communities. Animal species may host nitrogen-metabolizing microbes while phototrophs in the same environmental setting simultaneously compete for the animals' excreted ammonium. Light levels controlling phototroph ammonium uptake may thus mediate nitrogen transformations.

Stable isotope enrichment experiments are an established methodology for quantifying nitrogen processing in marine environments where the transfer of a tracer between source and product pools is measured over time (Glibert et al. 1982, Lipschultz 2008). Typically, these assays are done on seawater or sediments (e.g. review by Beman et al. 2011), though there are some examples where an organism is assayed (e.g. Heisterkamp et al. 2013). One acknowledged challenge of these experiments is the simultaneous occurrence of multiple processes that can dilute isotopically the source pool. For example, in a $^{15}NH_4$ tracer to estimate nitrification, the ammonium tracer could be diluted by the production of unlabeled NH_4^+ by remineralization or the microbial reduction of nitrite. Without accounting for isotope dilution, rates of transfer of NH_4^+ to other pools would accordingly be underestimated. To assess the importance of isotope dilution in our tidepool systems we compare rates of nitrogen transformation using two approaches: (1) Using the previously used source-product model for a single transformation from a ^{15}N-enriched source to a single product which does not account for isotope dilution (as discussed in Glibert et al. 1982, Lipschultz 2008), and (2) Using a set of 6 differential equations for modeling six different, simultaneous nitrogen processes which accounts for isotope dilution in all relevant pools as well as the passage of tracer into intermediate pools.

Here we quantify the influence of a common coastal marine animal, the California mussel, on the overall magnitude of and the partitioning between simultaneous nitrogen transformations, using tidepools at low tide as 'experimental mesocosms'. We use an experimental approach to test the possible interacting roles of this animal and light on the rates of nitrogen transformations that, in particular, influence net nitrogen retention. We manipulated the presence and absence of mussels

and light in combination with stable isotope tracer addition to directly test their effects on nitrogen transformations. Microbial nitrogen transformations estimated from differential equation models were much higher than published rates for which rate estimates are treated singularly. We use the experiment and model together to test whether nitrogen transformations in the tidepools are elevated by mussels, inhibited by light, or affected by other environmental variables. We also test for evidence of interactions between phototrophs and nitrogen-utilizing microbes.

2. Methods

2.1 A Model for experimental data

The fates of 3 forms of inorganic nitrogen (ammonium, nitrite, nitrate) in an isolated tidepool include a variety of processes mediated by microbes and other intertidal inhabitants, and are illustrated in Fig 1. For ammonium, increases in concentration (and dilution of an enriched tracer) can occur via excretion by animals and is represented by remineralization (m). Phototrophs, both prokaryotic and eukaryotic, can assimilate ammonium and nitrate leading to decreases in concentration, designated by uptake (u). Microbial transformations include ammonium oxidation to nitrite (h), nitrite oxidation to nitrate (x), nitrate reduction to nitrite (y), and nitrite reduction to ammonium (r). Remineralization, m, does not depend on any state variable, whereas the other parameters are first-order rate constants in which the rate is the product of the parameter and the appropriate concentration. Because they are the first steps toward denitrification (production of N_2), both nitrite and nitrate reduction should be favored under low oxygen conditions. Denitrification, in its entirety, and anammox (which combines ammonium and nitrite to produce N_2), are not explicitly modeled. Experiments to date that have

utilized gas-tight chambers have not detected nitrogen loss via N_2 gas production (unpublished data) and we thus assume that nitrate and nitrite reduction were incomplete with respect to N_2 production and consistent with nitrogen retention in the system.

The traditional source-product model generally involves estimating an average rate from time 0 to time t (Lipschultz 2008) and has the general form:

$$Rate = (R_k(t) - R_k(0))/[(R_s(0) - R_k(0)) * \Delta t] * [\bar{k}] \quad \text{Eq. (1)}$$

where k is the sink or product at time t (or the average $\bar{k}$), s is the source. Average product concentration over the source of the experiment is $\bar{k}$ and R designates the atom % ($^{15}N/(^{15}N + ^{14}N)$ x100) of either the source or product component at the beginning of the experiment (0) or the end (t). Equation (1) can be used to estimate individual nitrogen transformation rates assuming little change in R_k. For example, ammonium oxidation to nitrite (*h* in Fig 1) is estimated by adding $^{15}NH_4$ and monitoring the ^{15}N enrichment in nitrite. Nitrate reduction to nitrite (*y*) is estimated by adding $^{15}NO_3$, and monitoring the ^{15}N enrichment in nitrite.

A recognized shortcoming of Eq. (1) is that multiple simultaneous processes (e.g. Fig. 1) can change the concentration and isotopic composition of source and product nitrogen pools (Lipschultz 2008). Resolving the influence of multiple, contemporaneous nitrogen transformations requires a new approach that accounts for their influence over time on the distribution of ^{15}N tracer. Pather et al. (2014) used an isotope dilution model (Glibert et al. 1982) that included simultaneous ammonium remineralization and uptake. Here, we extend that approach by constructing a differential equation model that includes all six simultaneous processes described above. We then fit our model to observed time-dependent changes in the

concentrations and isotopic composition of ammonium, nitrite and nitrate. Because microbial metabolisms (*h, x, y, r*), phototroph uptake (*u*), and animal metabolism (*m*) should be occurring simultaneously, a major advantage of the differential equation model is that it estimates simultaneous multiple processes.

In our differential equation model (Fig. 1), three differential equations describe how the concentrations of ammonium [A], nitrite [Ni], and nitrate [Na] in nmol L^{-1} change with time as a function of the 6 nitrogen flux terms.

$$\frac{d[A]}{dt} = m + r[Ni] - h[A] - 2u[A] \qquad \text{(Eq. 2)}$$

$$\frac{d[Ni]}{dt} = h[A] + y[Na] - r[Ni] - x\,[Ni] \qquad \text{(Eq. 3)}$$

$$\frac{d[Na]}{dt} = x[Ni] - y[Na] - u[Na] \qquad \text{(Eq. 4)}$$

Ammonium remineralization (*m*) is assumed to be a constant rate independent of ammonium concentration. However, the other fluxes are first-order dependent on source concentrations with *h*, *u*, *r, x,* and *y* as the rate constants for ammonium oxidation, phototroph uptake, and nitrite reduction, nitrite oxidation, and nitrate reduction respectively. We also assumed that ammonium uptake (2*u*) was double that of nitrate uptake, a ratio reflecting the relative energetic ease of ammonium uptake by phototrophs (Thomas and Harrison 1985, Dortch 1990) and supported by measurements (Hurd et al. 2014). This 2:1 multiplier fit the data well across tidepool experiments (see below) and provided better fits than a higher or lower multiplier for ammonium:nitrate uptake. We note, however, that there are likely among species differences in *u* and its multiplier for ammonium uptake that need further study in marine macroalgae. By using only *u* to represent both phototrophic ammonium and nitrate uptake, we avoided an increase in

179 the number of parameters and we simplified our model fitting routine. Although we initially set *u*
180 to zero at night, we found that model fits were best when we let the model fit some phototrophic
181 uptake at night, a phenomenon consistent with the observation that dark photosynthesis via
182 carbon storage occurs in intertidal macroalgae (Kremer 1981). We excluded the uptake term (*u*)
183 from nitrite dynamics because nitrite is at much lower relative abundance compared with
184 ammonium and nitrate and is not known as a preferred nitrogen source for phototrophs. Finally,
185 we note that *u* could also include uptake by heterotrophic bacteria. Based on the results presented
186 below, however, phototrophic uptake appeared to dominate the *u* term. Given that nitrate and
187 nitrite reduction are favored only at low O_2 concentration, it might be presumed that reducing
188 processes are insignificant. However, tidepools with their natural complement of animals and
189 algae, sediment, and small nooks and crannies likely have a high degree of spatial heterogeneity
190 in oxygen and our results show significant rates of these processes.
191
192 Three equations model the time-varying concentrations (nmol $^{15}N\ L^{-1}$) of ^{15}N ammonium
193 (n15A), nitrite (n15Ni), and nitrate (n15Na). $^{15}NH_4$ is diluted over time by remineralization (*m*)
194 in the naturally occurring ratio of $^{15}NH_4$ to $^{14}NH_4$ of 0.00366. All other fluxes transfer ^{15}N from
195 source to product in proportion to total nitrogen transfer:

$$\frac{d[n15A]}{dt} = m(0.00366) + r[n15Ni] - h[n15A] - 2u[n15A] \qquad \text{(Eq. 5)}$$

$$\frac{d[n15Ni]}{dt} = h[n15A] + y[n15Na] - r[n15Ni] - x[n15Ni] \qquad \text{(Eq. 6)}$$

$$\frac{d[n15Na]}{dt} = x[n15Ni] - y[n15Na] - u[n15Na] \qquad \text{(Eq. 7)}$$

196 All parameter definitions are summarized in Table 1. Although isotope fractionation is known to
197 occur for these nitrogen transformations, their magnitude is small compared to experimental

198 enrichment values (e.g. Granger et al. 2008, Casciotti 2009, Granger et al. 2010, Swart et al
199 2014). We thus assumed that fractionation was insignificant in the context of this experimental
200 manipulation and that first order reaction rate coefficients were equivalent for ^{14}N and ^{15}N
201 containing forms of DIN.
202
203 We solved Eqs. 2-7 for the 6 parameters (*m, u, h, x, r, y*) simultaneously, by finding the best fits
204 to the concentration and ^{15}N data for each experimental tidepool (see Sect 2.3). We further
205 leveraged this experimental approach by comparing results for experiments carried out during
206 the day and at night, and in tidepools with and without mussels, generating multiple parameter
207 estimates and analyzing how they varied with environmental variables. To do so, we conducted
208 all 4 experimental variants in each tidepool over the course of 2 months (daytime $^{15}NH_4$,
209 nighttime $^{15}NH_4$, daytime $^{15}NO_3$, nighttime $^{15}NO_3$) (see Methods below).
210
211 **2.2 Isotope enrichment experiments in tidepools**
212 All isotope enrichment experiments were done in tidepools at Second Beach, a rocky north-
213 facing bench 2 km east of Neah Bay, WA, USA (48°23' N, 124° 40' W) within the Makah Tribal
214 Reservation. The experimental methods were described in the Pather et al (2014), but are briefly
215 reviewed here. Since 2002, California mussels (*Mytilus californianus*) have been removed from
216 5 tidepools while 5 others have remained as controls; in the year of this study, mussels were
217 hand-removed (by cutting byssal threads) a month prior to the experiment to eliminate any
218 biogeochemical signal of our presence. Besides this single perturbation, the pools have been left
219 intact and contain a natural assemblage of macroalgae, microphytobenthos, surfgrasses
220 *Phyllospadix scouleri* and *P. serrulatus* and macrofauna such as limpets, anemones, and fishes;

221 the tidepools were 1.2 to 1.5 m above Mean Lower Low Water (MLLW) (Pfister 2007). The
222 isolation of these tidepools for 5 to 6 hours during the low tide excursions both during daylight
223 and nighttime hours during the summer of 2010 made it ideal to use the tidepools as intact
224 mesocosms and probe the nitrogen transformations in natural ecosystems. Here we extend the
225 analysis of Pather et al. (2014) by quantifying nitrogen cycling that is due to microbial
226 transformations. We also augment their ^{15}N ammonium addition results with results for ^{15}N
227 nitrate addition.
228
229 Four ^{15}N enrichment experiments within these 2 groups of tidepools provided a test of the fate of
230 ammonium and nitrate, as a function of day and night hours (e.g. with and without
231 photosynthesis), and the presence and absence of animals. The 'δ' notation is standard for
232 expressing relatively low levels of ^{15}N enrichment as well as variations in natural abundance ^{15}N
233 ($\delta^{15}N‰=[(R_{sample}-R_{atmN2})/R_{atmN2}]$ x 1000) and is used here for expressing measured values. For
234 model calculations, $\delta^{15}N$ values were first converted to $^{15}N/^{14}N$ ratios and then to the
235 concentration of ^{15}N by multiplying by the corresponding nutrient concentration. The four
236 enrichment experiments included a target 1000‰ enrichment of either $\delta^{15}NH_4$ (added as 0.05M
237 ammonium chloride, $^{15}NH_4Cl$) or $\delta^{15}NO_3$ (added as 0.05M sodium nitrate, $Na^{15}NO_3$), thus
238 doubling either the $^{15}N\text{-}NH_4^+$ or $^{15}N\text{-}NO_3^-$ concentration during both a daytime low tide (25 Jun
239 2010, ~0715 to 1245 and 27 Jun 2010, ~0730 to 1300h), and a nighttime low tide (~2000 to
240 0145h on 13-14 Aug 2010 and 2150 to 0400h on 15-16 Aug 2010). Although only 2 days
241 separated the daytime ammonium and nitrate experiments, high tide flushed these areas 3 times
242 and our initial samples for the nitrate enrichment experiment corrected for any residual ^{15}N. A
243 six-week interval between daytime and nighttime experiments was necessary due to the timing of

low tides in the region. Strong nighttime low tide excursions only occurred in August, while daytime spring tides are ideal in June. These two experimental timepoints showed similar starting tidepool seawater temperatures (11.4 in Jun versus 11.3^{o}C in Aug) and similar DIN concentrations (20.0 and 23.1 μmolL^{-1}). Both ammonium and nitrate concentrations in tidepools are typically high (>10 μmolL^{-1}) minimizing any concentration-related effects from tracer addition. Tidepool volume had been estimated previously with addition of a known amount of blue food coloring (e.g. Pfister 1995) and averaged 57.1 L with a range of 26.1 to 97.4 L. Deviations in our target of 1000‰ initial enrichment occurred due to natural variation in nutrient concentrations at the time of tracer addition, as well as error in tidepool volume estimates.

In all experiments, a water sample prior to tracer addition was collected to verify natural abundance isotope levels (T_o). After tracer solution was added and stirred, a sample of water was immediately taken to estimate actual initial enrichment (T_1). A second sample was taken ~ 2 h later (T_2), followed by a final sample after ~5 h (T_3), resulting in 3 samples to estimate the time course of concentration and ^{15}N enrichment in NH_4^+, NO_2^-, and NO_3^- in tidepool water. Although it would have been ideal to have greater than 4 samples to precisely describe the time course of ^{15}N through time, this number represented a cost-effective number across ten replicate tidepools and four experiments, and minimized investigator disturbance during the experiment. For each sample, we filtered ~180 ml of tidepool water through a syringe-filter (Whatman GF/F) into HDPE bottles, which we kept frozen until analysis. All nutrient concentrations were analyzed at the University of Washington Marine Chemistry lab, while isotope determinations were done at University of Massachusetts, Dartmouth. Methodology for nutrient and isotopic composition was reported previously (Pather et al. 2014, Pfister et al. 2014a). Briefly, nitrogen stable isotopes of

ammonium were measured according to a modified version of the NH_4 oxidation method detailed in Zhang et al. (2007). NH_4 is oxidized to nitrite using a hypobromite solution and then reduced to N_2O using a sodium azide-acetic acid reagent before analysis on an IRMS (isotope ratio mass spectrometer). The stable isotope ratios of nitrate were measured by cadmium reduction to nitrite, followed by reaction with azide to N_2O (McIlvin and Altabet 2005). Nighttime sampling was done using headlamps, and took only 2-5 min, resulting in negligible illumination near tidepools. Tidepool oxygen, pH and temperature (Hach HQ4D) were also collected at ~ 2 h intervals throughout the experiment, and all tidepools had a HOBO temperature logger recording at 10 min intervals.

2.3 Fitting the Differential Equation Model to Data

Each tidepool experiment had 3 time points for nitrogen isotope composition and concentration, making it possible to fit our model to the data for each experiment. We solved our differential equations using the 'ode' function of R (in the deSolve R package, Version 3.1.0, www.r-project.org, Soetaert et al. 2012). The fit of our model to the data was calculated with the 'modCost' function of the FME package, which calculates the sum of the squared errors between the model and the data. We fit the model to the data using the 'modFit' function that uses a Levenberg-Marquardt minimization algorithm (Soetaert et al. 2010). As we did this estimation for each experiment, not treatment averages, we were able to examine stoichiometric relationships between nitrogen fluxes maintained at the scale of individual tidepools. Although the fitting routine always converged, we further tested the robustness of the fitting routine in several ways. First, we randomly varied the initial values for the parameters 100 times, drawing initial values from uniform distributions that allowed the parameter estimates to vary over

several orders of magnitude (between 0 to 10). Because the *m* parameter was not first order and logically could be large, it ranged from 0 through 10^6. In all cases, the sum of squares of at least the best 10 parameter sets were within 10^{-3} (or less than 1-3% different), strongly suggesting that our fitting routine found the best parameter sets. As a second test of the model, we calculated net production or loss of ^{15}N by comparing the resulting total moles of ^{15}N from the observed values in each tidepool at the end of each experiment to the corresponding best-fit parameter estimates.

Finally, we compared our differential equation model with the source-product model shown in Eq. (1). Because our tracer experiments had 3 time points (T_1, T_2, T_3), we used the interval from T_1 to T_2 to estimate the first paths for the transfer of tracer via oxidation or reduction (*h* and *y*) and the interval from T_2 to T_3 to estimate the second oxidation or reduction process (*x* and *r*). In this way, there was time for the tracer to become incorporated into nitrite before we estimated the transformation rates of nitrite oxidation (*x*) in the case of enriched ammonium addition, or reduction (*r*) in the case of enriched nitrate addition. Focusing our source-sink estimation on these intervals allowed us to produce the most accurate rate estimates from the source-sink model.

We measured multiple responses in our experimental manipulation. We analyzed all responses with a linear mixed effects model using tidepool as a random effect and testing for a statistical interaction between mussel presence and light (R, www.r-project.org).

3. Results

3.1 Isotope Patterns in experiments

After approximately 5 to 6 hours of isolation at low tide, results were dependent on both the presence of mussels and the availability of sunlight (Fig. 2, Table 2). Ammonium concentration was overall greater with mussels and during the day, and oxygen, temperature and pH all tended to be greater during the day. Tidepool pH was lower at night ($p<0.05$) and possibly lower with mussels ($0.10<p<0.05$). The dynamics of $\delta^{15}N_{NH4}$, $\delta^{15}N_{NO2,}$ and $\delta^{15}N_{NO3}$ over the course of the experiment revealed transfer of the tracer isotope and thus the action of microbial nitrogen transformations. When $^{15}N\text{-}NH_4^+$ was added, enrichment in $\delta^{15}N_{NO2,}$ and $\delta^{15}N_{NO3}$ was seen, though the presence of mussels diluted the $\delta^{15}N_{NH4}$ signal. Similarly, enrichment in $\delta^{15}N_{NH4}$ and $\delta^{15}N_{NO2}$ followed the addition of $^{15}N\text{-}NO_3^-$ (Appendix A1).

3.2 The differential equation model estimates nitrogen transformation rates

The advantage of using our tidepool experiments is that they contain the full range of actual biological components and environmental fluctuations; but as they vary in the composition of these components they also show individual differences. We thus fit the model to each tidepool individually, rather than a mean value, allowing any influences due to environmental differences to be incorporated into parameter estimates. ODE model predictions were generally highly concordant with the observed nutrient and isotope data measured for each tidepool experiment (Fig. 3). Our estimates of u assumed that phototrophic ammonium uptake was twice that of nitrate uptake, an assumption that generally fit the observed data well (Appendix A2). In addition to providing a good visual fit to the data for each tidepool (Fig. 3), the estimated parameters predicted well the total amount of ^{15}N measured at the end of the experiment (Fig. 4). Individual results deviated by as much as $\pm$20 nmol L^{-1}, but the estimated and measured quantities were very similar and indicated the model showed no bias toward producing or consuming ^{15}N (Fig.

3). The mean ^{15}N was 122.3 nmol total in the ammonium enrichment experiments and 158.6 total in the nitrate enrichment experiments, indicating that deviations were relatively modest (<16%), especially given the multiple sources of variability in collecting and analyzing tidepool seawater.

3.3 The significant effect of mussels and light on nitrogen processing

The rates of ammonium remineralization in tidepools that we estimated with our ODE model were greatest during the day when mussels were present, as was the uptake of ammonium (Fig. 2). In turn, all nitrogen metabolisms showed the greatest rates in the presence of mussels (Fig. 5, Table 3, Table 4). Further, all nitrogen transformations were greatest during the day with the exception of nitrate reduction. For ammonium and nitrite oxidation (*h*A and *x*Ni), rates increased an order of magnitude in the presence of mussels and during the day. As with all the microbial transformations, nitrogen uptake attributed to all photosynthesizing species, from microalgae to macroalgae and seagrasses, was greatest with mussels and also during the day. When we tallied the percentage of ammonium flux due to microbes (nitrification + nitrite reduction) relative to all the ammonium flux per tidepool ($(h\bar{A}+r\bar{N}\imath)/(h\bar{A}+r\bar{N}\imath+2u)$, Table 3), we found that microbial ammonium flux accounted for 32% of all ammonium flux when mussels were present and it was daylight. Similarly, microbial nitrate flux was 61.4% of all nitrate flux. Although inorganic nitrogen concentrations were always greater with mussels (Fig. 2), the rates of nitrogen transformations we estimated were greatly affected by time of day and mussels (Figs. 2, 5, statistical summary in Table 4).

3.4 Comparing the ODE model to single rate, source-sink models

All rates of nitrogen transformation during the day and with mussels estimated with our differential equation model (Eqs. 2-7) were greater than estimated by the traditional source-product model (Fig. 5, Table 4). The ODE model always produced an estimate of the ammonium oxidation rate far greater than that of the source-product model, particularly during the day. The ammonium oxidation rate estimated with our differential equation model was uncorrelated with the estimates from the source-product model (Spearman's r=0.004, Table 4). Overall, there was little concordance between microbial nitrogen transformations estimated with the ODE model and the source-product model, as the ODE model frequently estimated higher rates (Fig. 5, Table 3).

3.5 Inferences about the relationships among nitrogen processes

Parameter estimates from our model allowed us to assess the potential interaction among nitrogen processes. We tested how model estimates of photosynthetic versus microbial chemolithotrophic nitrogen use were related. If competition for ammonium occurs, then ammonium oxidation (h) could be negatively related to phototrophic ammonium uptake ($2u$). To avoid correlating parameters estimated simultaneously from the same model fitting attempt, we correlated ammonium oxidation (hA) from the $^{15}NH_4$ enrichment with the uptake (u) from the $^{15}NO_3$ experiments (and vice versa) and did not find a significant relationship in either case (r=0.320, p=0.169 and r=0.297, p=0.200). The significant and positive relationship between ammonium oxidation (hA) and remineralization (m) estimated from our differential equation model (0.656, p<0.001) could be biologically driven. However, there are numerous reasons for underlying relationships between model parameters. As further evidence that there is an underlying statistical correlation between ammonium oxidation and remineralization, we note

that ammonium oxidation in our ODE model was also positively related to animal remineralization estimated independently, using the simple isotope dilution model from Pather et al. (2014) ($r=0.687$, $p<0.001$). The positive relationship was unaffected by day or night, indicating no enhancement of ammonium oxidation when photosynthetic ammonium uptake was minimized.

Finally, we found few correlations between nitrogen transformation rates and oxygen, temperature and pH in tidepools at the end of the low tide period. Only remineralization and nitrogen uptake rates show a positive correlation with higher temperatures ($r=0.423$, $p=0.009$ & $r=0.432$, $p=0.008$, respectively), primarily eukaryotic metabolic processes that increased with temperature.

4. Discussion

4.1 Animal and microbial contributions to nitrogen transformations

The remineralization of ammonium, oxidation and reduction of inorganic nitrogen, and the uptake of ammonium and nitrate were all greater in tidepools with mussels versus those where mussels were removed. Mean nitrate flux due to microbial processing (the sum of microbial nitrate transformations in Table 3) ranged from 8 to 61% of the total nitrate uptake attributed to both microbes and phototrophs, with the highest values when mussels were present and it was daylight. Microbial processing accounted for an average 32% of the total ammonium flux with mussels and daylight. Processing of both nitrate and ammonium by microbial chemolithotrophs was thus significant in this rocky shore environment, and especially so when mussels were

present. Previous analysis of ammonium uptake in this system indicated that suspended particles (e.g. phytoplankton) in tidepool seawater account for a negligible amount of ammonium uptake (only 1-3 nmol L^{-1} h^{-1}) and microbial activity in tidepool seawater was an order of magnitude less than benthic microbial activity (Pather et al. 2014). Additionally, benthic algae uptake rates (estimated at ~5 x 10^{-4} h^{-1}, Pather et al. 2014) likely dominate the parameter *u*, though the biomass specific uptake rates for the algae in our tidepools are unknown because we would have had to destructively sample all algae to estimate this. However, published rates of ammonium uptake in red algae ranged from 15900-62000 nmol per hour for every gram of algal dry weight, while those for nitrate are 9700-28500 (Hurd et al. 2014). Thus, several individual algae could account for the uptake of nitrogen that is not microbial, and our estimates of uptake using the *u* parameter in the model are consistent with literature values (Table 3). In total, our enrichment experiments indicate that microbial transformations can be as great as and even exceed the contributions of phototrophs to nitrogen dynamics. Further, the microbial activity related to nitrogen cycling is primarily in association with benthic animals and phototrophs.

Previous genomic analyses showed that inert substrates (e.g. rocks) in tidepools with mussels host a nearly identical microbial community to those in tidepools without mussels (Pfister et al. 2014b), while mussel shells themselves host a rich diversity of nitrogen-metabolizing microbial taxa (Pfister et al. 2010). Combined with the nitrogen processing rates we quantified here, these studies suggest that California mussels are loci for the microbial processing of nitrogen. Marine invertebrates as hosts for significant nitrogen processing is further supported by work with snails and other bivalves, which are demonstrated sites of nitrogen transformations including ammonium oxidation (Welsh and Castadelli 2004, Stief et al. 2013, Heisterkamp et al. 2013).

428 N_2O production is also suggested for sediment-dwelling bivalves (Heisterkamp et al. 2013) and
429 those in sealed chambers (Stief et al. 2009). Evidence for bivalves as hotspots for nutrient
430 dynamics also includes species in river and stream environments (Atkinson & Vaughn 2014).
431 Mussels on rocky shores can average very high densities of 4661 individuals per m^2 (Suchanek
432 1979), suggesting that ammonium concentrations above mussels should be in mmol
433 concentrations (Pfister et al. 2010). The observation of concentrations much lower than mmol
434 quantities directly over mussel beds (Aquilino et al. 2009), and in tidepools (this study) suggests
435 multiple N processing pathways as observed here.
436
437 **4.2 Microbes contribute to nitrogen retention**
438 In high-energy coastal environments, animal regenerated ammonium could be advected by
439 waves and currents rather than retained. Because the rates we quantified are rapid, and because
440 tidepool habitats are high flow refugia, net retention of inorganic nitrogen in nearshore areas can
441 result, a phenomenon that is likely to enhance local primary production. Over a diel cycle, both
442 ammonium and nitrite oxidation and nitrate and nitrite reduction occurred, and all are processes
443 that retain dissolved and biologically available nitrogen. Although we did not follow our tracer
444 into all tidepool species, previous analyses showed it was readily incorporated into tidepool algae
445 (Pather et al. 2014). Nitrogen loss processes were not quantified, though other experiments with
446 gas-tight chambers indicated no loss of nitrogen via enriched N_2 gas (Pfister & Altabet
447 unpublished data). Additionally, if the loss of ^{15}N signal was occurring due to anammox or
448 denitrification completed to nitrogen gas, then our models would have systematically estimated a
449 loss of ^{15}N, a result not supported by our analyses (Fig. 4). Further, phototrophic uptake of ^{15}N
450 was the only other term in the model for nitrogen loss. Our model predictions for uptake not only

were robust in both day and night experiments (Fig. 4), but the uptake rates were highly consistent with measured uptake rates of marine algae (see section 4.1 above). We recognize, however, that nitrogen loss processes via the production of the greenhouse gas nitrous oxide is suggested in association with other animal species (Heisterkamp et al. 2013). Though the return of nitrogen gas to the atmosphere is a significant feature of low oxygen, open ocean areas (Ward 2013) there was no evidence for it here. In this study, and in the analysis of naturally occurring nitrogen isotopes (Pfister et al. 2014), nitrogen retention is instead suggested in high-energy coastal areas, though the generality of this finding deserves further study.

Both nitrate and nitrite reduction rates were significant and are evidence for incomplete denitrification or DNRA processes thought to be occurring only at low oxygen. Even during daytime periods of high oxygen, nitrate and nitrite reduction were observed, suggesting that tidepools provide microsites where these microbial reducing processes can take place. The oxidation of ammonium and nitrite, though not positively related to final oxygen level, was greatest during the day and with mussels. Even at night when oxygen could be very low, there was sufficient ambient oxygen to permit nitrification. Thus, even though remineralization decreased at night and oxygen levels dropped, presumably associated with decreased mussel metabolism, ammonium oxidation remained at an average of 160.6 nmol L^{-1} h^{-1} in the presence of mussels.

Although competition for ammonium between nitrifiers and phototrophs is poorly understood, the preference for ammonium uptake may make it a contested resource. Sediment microalgae have been shown to be competitively superior to ammonium oxidizing bacteria, likely due to

474 higher specific uptake rates and faster growth (Risgaard-Petersen et al. 2004). Here, we found
475 little evidence for competitive interactions for either ammonium or nitrate between
476 photosynthetic processes and microbial chemolithotrophs. Microbial transformations in the dark
477 did not increase, suggesting that microbial nitrogen metabolism is driven more by the stimulation
478 of animal excretion that occurs in these tidepools during the day, perhaps because of increased
479 tidepool temperature (Bayne & Scullard 1977). We also show no evidence of UV inhibition of
480 nitrification (e.g. Horrigan & Springer 1990, Guerrero & Jones 1995). We note also that
481 tidepool ammonium levels rarely were lower than several μM, and thus ammonium should not
482 have been depleted and limiting unless there are depleted microsites. Further studies at low
483 ammonium, including areas where animal regeneration is reduced and ammonium may be
484 contested, are warranted to understand how phototrophs and chemolithotrophs interact.
485
486
487 **4.3 The Differential equation model captures rapid and simultaneous processes**
488 We developed the ODE model to simultaneously estimate multiple microbial transformation
489 rates which provide a more realistic descriptor of microbial activity in nature. Our model focus
490 on the rates of simultaneous nitrogen transformations assures that it is general and applicable to
491 any system. A key result here is that rate estimates from the differential equation model were
492 often much greater than those from the source-product model (Lipschultz 2008, and Glibert
493 1982). We suggest two reasons that our ODE estimated greater rates. First, the rapidity of
494 microbial transformations combined with the diversity of microsites in nature mean that tracer
495 enrichment can readily cycle through multiple products. Thus, ^{15}N in ammonium may be
496 oxidized not only to nitrite, but also to nitrate and then potentially reduced (Fig. 1). Our model

allows this 'cycling', whereas a source-sink model assumes a single source and product are involved in the estimation of ^{15}N dynamics. The second reason our ODE model estimates greater rates than a source-sink is that ammonium remineralization by macrobiota in nature can rapidly dilute the $^{15}NH_4^+$ signal. A diluted $^{15}NH_4^+$ signal leads to underestimation of nitrogen dynamics with source-sink models, a concern noted by its authors when source-product models were derived. Here, and in Pather et al. (2014), we note that the effects of ammonium dilution were most pronounced with mussels during the day, where all microbial rates were underestimated with a source-product model. Our ODE model, in contrast, accounts for the propagation of tracer dilution by ammonium remineralization to all DIN pools, likely resulting in greater estimates for multiple nitrogen metabolisms. Indeed, our estimates of nitrification are several orders of magnitude greater than those estimated in other coastal locales with source-product models (Beman et al. 2011), allowing us to conclude that macrobiota greatly enhance rates of nitrogen transformations. We further note that the rates we quantified are characterized by high variability among tidepools, a result likely due to both measurement error for ^{15}N enriched field samples, but also from natural variability in space and time for processes sensitive to species composition and environmental factors.

5. Conclusions

Tidepools demonstrated a range of prokaryotic and eukaryotic nitrogen metabolisms that varied with animal presence and the time of day, echoing other recent studies that demonstrate marine animals serve as sites for a diversity of nitrogen metabolisms (Fiore et al. 2010, Heisterkamp et al. 2013). The ubiquity in the coastal environment of the flora and fauna found in tidepools suggests that microbial nitrogen transformations are not unique to tidepools but a general feature

520 associated with macrobiota. The relatively high variability in the estimates of all microbial
521 nitrogen transformations we documented is paralleled by variability in the environmental
522 variables (e.g. oxygen, pH, temperature, species composition) that may also foster a rich mosaic
523 of tidepool microsites for microbial biogeochemical processing and nitrogen regeneration and
524 retention. Scaling up to the entire rocky shore ecosystem suggests a large potential role for
525 animals in ameliorating fluctuations in upwelling and nutrient delivery. Meanwhile, ongoing
526 animal harvest in ocean systems has greatly impacted nitrogen cycling (e.g. Maranger et al.
527 2008), making it imperative to understand the links between nitrogen in coastal systems and
528 animal harvest.
529
530 *Author Contribution.* CAP, MA, SP designed the experiments and CAP, MA, SP carried them
531 out and did laboratory analyses. CAP, GD, MA developed the model. CAP prepared the
532 manuscript with contributions from all co-authors.
533
534 *Acknowledgements.* We thank E. Altabet, S. Betcher, B. Colson, M. Kanichy, O. Moulton, P.
535 Zaykowski for making the field experiment a success, including R. Belanger's lab efforts. K.
536 Krogsland provided nutrient analyses and J. Larkum laboratory isotope expertise. We thank the
537 Makah Nation for access. Funding was provided by NSF-OCE 09-28232 (CAP), NSF-OCE 09-
538 28152 (MAA), and a Fulbright Foreign Student Award (SP).
539
540 **References**

Allgeier, J. E., Layman, C. A., Mumby, P. J. and Rosemond, A. D.: Consistent nutrient storage and supply mediated by diverse fish communities in coral reef ecosystems, Global Change Biology, 20(8), 2459–2472, doi:10.1111/gcb.12566, 2014.

Aquilino, K. M., Bracken, M. E. S., Faubel, M. N. and Stachowicz, J. J.: Local-scale nutrient regeneration facilitates seaweed growth on wave-exposed rocky shores in an upwelling system, Limnology and Oceanography, 54(1), 309–317, doi:10.4319/lo.2009.54.1.0309, 2009.

Atkinson, C. L. and Vaughn, C. C.: Biogeochemical hotspots: temporal and spatial scaling of the impact of freshwater mussels on ecosystem function, Freshw Biol, 60(3), 563–574, doi:10.1111/fwb.12498, 2015.

Bayne, B. L. and Scullard, C.: Rates of nitrogen excretion by species of *Mytilus* (Bivalvia: Mollusca), Journal of the Marine Biological Association of the United Kingdom, 57(2), 355–369, doi:10.1017/S0025315400021809, 1977.

Beman, J. Michael, Chow, Cheryl-Emiliane, King, Andrew, Feng, Yuanyuan, Fuhrman, Jed A., Andersson, Andreas and Bates, Nicholas R.: Global declines in ocean nitrification rates as a consequence of ocean acidification., Proceedings of the National Academy of Sciences, 108, 208–213, 2011.

Bracken, M. E. S.: Invertebrate-mediated nutrient loading increases growth of an intertidal macroalga, Journal of Phycology, 40(6), 1032–1041, doi:10.1111/j.1529-8817.2004.03106.x, 2004.

Casciotti, K. L.: Inverse kinetic isotope fractionation during bacterial nitrite oxidation, Geochimica et Cosmochimica Acta, 73(7), 2061–2076, doi:10.1016/j.gca.2008.12.022, 2009.

Dortch, Q.: The interaction between ammonium and nitrate uptake in phytoplankton, , 61, 183–201, 1990.

564 Dugdale, R. and Goering, J.: Uptake of new and regenerated forms of nitrogen in primary
565 productivity, Limnology and Oceanography, 12(2), 196–206, 1967.
566 Fiore, C. L., Jarett, J. K., Olson, N. D. and Lesser, M. P.: Nitrogen fixation and nitrogen
567 transformations in marine symbioses, Trends in Microbiology, 18(10), 455–463,
568 doi:10.1016/j.tim.2010.07.001, 2010.
569 Fowler, D., Coyle, M., Skiba, U., Sutton, M. A., Cape, J. N., Reis, S., Sheppard, L. J., Jenkins,
570 A., Grizzetti, B., Galloway, J. N., Vitousek, P., Leach, A., Bouwman, A. F., Butterbach-Bahl,
571 K., Dentener, F., Stevenson, D., Amann, M. and Voss, M.: The global nitrogen cycle in the
572 twenty-first century, Philosophical Transactions of the Royal Society of London B: Biological
573 Sciences, 368(1621), 20130164, doi:10.1098/rstb.2013.0164, 2013.
574 Galloway, J. N., Townsend, A. R., Erisman, J. W., Bekunda, M., Cai, Z., Freney, J. R.,
575 Martinelli, L. A., Seitzinger, S. P. and Sutton, M. A.: Transformation of the nitrogen cycle:
576 recent trends, questions, and potential solutions, Science, 320(5878), 889–892,
577 doi:10.1126/science.1136674, 2008.
578 Glibert, Pamela M., Lipschultz, F., McCarthy, James J. and Altabet, M. A.: Isotope dilution
579 models of uptake and remineralization of ammonium by marine plankton, Limnology and
580 Oceanography, 27, 639–650, 1982.
581 Granger, J., Sigman, D. M., Lehmann, M. F. and Tortell, P. D.: Nitrogen and oxygen isotope
582 fractionation during dissimilatory nitrate reduction by denitrifying bacteria, Limnol.
583 Oceanogr., 53(6), 2533–2545, doi:10.4319/lo.2008.53.6.2533, 2008.
584 Granger, J., Sigman, D. M., Rohde, M. M., Maldonado, M. T. and Tortell, P. D.: N and O
585 isotope effects during nitrate assimilation by unicellular prokaryotic and eukaryotic plankton

cultures, Geochimica et Cosmochimica Acta, 74(3), 1030–1040, doi:10.1016/j.gca.2009.10.044, 2010.

Guerrero, M. A. and Jones, R. D.: Photoinhibition of marine nitrifying bacteria: wavelength-dependent response., Mar Ecol Prog Ser, 141, 183–192, 1995.

Heisterkamp, I. M., Schramm, A., Larsen, L. H., Svenningsen, N. B., Lavik, G., de Beer, D. and Stief, P.: Shell biofilm-associated nitrous oxide production in marine molluscs: processes, precursors and relative importance: Nitrous oxide production in shell biofilms, Environmental Microbiology, 15(7), 1943–1955, doi:10.1111/j.1462-2920.2012.02823.x, 2013.

Horrigan, S. G. and Springer, A. L.: Oceanic and estuarine ammonium oxidation: Effects of light, Limnology and Oceanography, 35(2), 479–482, doi:10.4319/lo.1990.35.2.0479, 1990.

Hurd, C. L., Harrison, P. J., Bischof, K. and Lobban, C. S.: Seaweed ecology and physiology, Second edition., Cambridge University Press, Cambridge ; New York., 2014.

Kremer, B. P.: Metabolic implications of non-photosynthetic carbon fixation in brown macroalgae, Phycologia, 20(3), 242–250, doi:10.2216/i0031-8884-20-3-242.1, 1981.

Lipschultz, F.: Isotope tracer methods for studies of the marine nitrogen cycle, in Nitrogen in the Marine Environment (2nd Edition), edited by D. G. Capone, D. A. Bronk, M. R. Mulholland, and E. J. Carpenter, pp. 1345–1384, Academic Press, San Diego. [online] Available from: http://www.sciencedirect.com/science/article/pii/B9780123725226000311 (Accessed 19 May 2014), 2008.

Magalhaes, C. M., Bordalo, A. A. and Wiebe, W. J.: Intertidal biofilms on rocky substratum can play a major role in estuarine carbon and nutrient dynamics, Mar Ecol Prog Ser, 258, 275–281, doi:10.3354/meps258275, 2003.

Maranger, R., Caraco, N., Duhamel, J. and Amyot, M.: Nitrogen transfer from sea to land via commercial fisheries, Nature Geosci, 1(2), 111–112, doi:10.1038/ngeo108, 2008.

McIlvin, M. R. and Altabet, M. A.: Chemical conversion of nitrate and nitrite to nitrous oxide for nitrogen and oxygen isotopic analysis in freshwater and aeawater, Analytical Chemistry, 77(17), 5589–5595, doi:10.1021/ac050528s, 2005.

Miranda, L. N., Hutchison, K., Grossman, A. R. and Brawley, S. H.: Diversity and abundance of the bacterial community of the red macroalga *Porphyra umbilicalis*: did bacterial farmers produce macroalgae?, edited by J. Neufeld, PLoS ONE, 8(3), e58269, doi:10.1371/journal.pone.0058269, 2013.

Moulton, O. M., Altabet, M. A., Beman, J. M., Deegan, L. A., Lloret, J., Lyons, M. K., Nelson, J. A. and Pfister, C. A.: Microbial associations with macrobiota in coastal ecosystems: patterns and implications for nitrogen cycling, Frontiers in Ecology and the Environment, 14(4), 200–208, doi:10.1002/fee.1262, 2016.

Pather, S., Pfister, C. A., Post, D. M. and Altabet, M. A.: Ammonium cycling in the rocky intertidal: Remineralization, removal, and retention, Limnology and Oceanography, 59(2), 361–372, doi:10.4319/lo.2014.59.2.0361, 2014.

Pfister, C. A.: Estimating competition coefficients from census data: a test with field manipulations of tidepool fishes, The American Naturalist, 146(2), 271–291, 1995.

Pfister, C. A.: Intertidal invertebrates locally enhance primary production, Ecology, 88(7), 1647–1653, doi:10.1890/06-1913.1, 2007.

Pfister, C. A., Meyer, F. and Antonopoulos, D. A.: Metagenomic profiling of a microbial assemblage associated with the California mussel: A node in networks of carbon and nitrogen

cycling, edited by R. DeSalle, PLoS ONE, 5(5), e10518, doi:10.1371/journal.pone.0010518, 2010.

Pfister, C. A., Altabet, M. A. and Post, D.: Animal regeneration and microbial retention of nitrogen along coastal rocky shores, Ecology, 95(10), 2803–2814, doi:10.1890/13-1825.1, 2014a.

Pfister, C. A., Gilbert, J. A. and Gibbons, S. M.: The role of macrobiota in structuring microbial communities along rocky shores, PeerJ, 2, e631, doi:10.7717/peerj.631, 2014b.

Plaganyi, E. E. and Branch, G. M.: Does the limpet Patella cochlear fertilize its own algal garden?, Marine Ecology Progress series, 194, 113–122, 2000.

Risgaard-Petersen, N., Nicolaisen, M. H., Revsbech, N. P. and Lomstein, B. A.: Competition between ammonia-oxidizing bacteria and benthic microalgae, Appl. Environ. Microbiol., 70(9), 5528–5537, doi:10.1128/AEM.70.9.5528-5537.2004, 2004.

Schindler, D. E., Knapp, R. A. and Leavitt, P. R.: Alteration of nutrient cycles and algal production resulting from fish introductions into mountain lakes, Ecosystems, 4(4), 308–321, doi:10.1007/s10021-001-0013-4, 2001.

Soetaert, K., Petzoldt, T. and Dresden, T. U.: Inverse modelling, sensitivity and Monte Carlo Analysis in R using package FME, Journal of Statistical Software, 33(3), 2010.

Soetaert, K., Cash, J. and Mazzia, F.: Solving Differential Equations in R, Springer Berlin Heidelberg, Berlin, Heidelberg. [online] Available from: http://link.springer.com/10.1007/978-3-642-28070-2 (Accessed 14 May 2015), 2012.

Stief, P.: Stimulation of microbial nitrogen cycling in aquatic ecosystems by benthic macrofauna: mechanisms and environmental implications, Biogeosciences, 10(12), 7829–7846, doi:10.5194/bg-10-7829-2013, 2013.

Stief, P., Poulsen, M., Nielsen, L. P., Brix, H. and Schramm, A.: Nitrous oxide emission by aquatic macrofauna, Proceedings of the National Academy of Sciences, 106(11), 4296–4300, doi:10.1073/pnas.0808228106, 2009.

Subalusky, A. L., Dutton, C. L., Rosi-Marshall, E. J. and Post, D. M.: The hippopotamus conveyor belt: vectors of carbon and nutrients from terrestrial grasslands to aquatic systems in sub-Saharan Africa, Freshw Biol, 60(3), 512–525, doi:10.1111/fwb.12474, 2015.

Suchanek, Thomas H.: The *Mytilus californianus* community: studies on the composition, structure, organization and dynamics of a mussel bed., University of Washington, Seattle, PhD Thesis., 1979.

Swart, P. K., Evans, S., Capo, T. and Altabet, M. A.: The fractionation of nitrogen and oxygen isotopes in macroalgae during the assimilation of nitrate, Biogeosciences, 11(21), 6147–6157, doi:10.5194/bg-11-6147-2014, 2014.

Taylor, R. B. and Rees, T. A. V.: Excretory products of mobile epifauna as a nitrogen source for seaweeds, Limnology and Oceanography, 43(4), 600–606, doi:10.4319/lo.1998.43.4.0600, 1998.

Thomas, T. E. and Harrison, P. J.: Effect of nitrogen supply on nitrogen uptake, accumulation and assimilation in *Porphyra perforata* (Rhodophyta), Marine Biology, 85(3), 269–278, doi:10.1007/BF00393247, 1985.

Vanni, M. J.: Nutrient cycling by animals in freshwater ecosystems, Annual Review of Ecology and Systematics, 33(1), 341–370, doi:10.1146/annurev.ecolsys.33.010802.150519, 2002.

Ward, B. B.: Nitrification, in Nitrogen in the Marine Environment, edited by D. G. Capone, D. A. Bronk, M. R. Mulholland, and E. J. Carpenter, pp. 199–262, Elsevier, Amsterdam., 2008.

Welsh, D. T. and Castadelli, G.: Bacterial nitrification activity directly associated with isolated benthic marine animals, Marine Biology, 144(5), 1029–1037, doi:10.1007/s00227-003-1252-z, 2004.

Worm, B., Barbier, E. B., Beaumont, N., Duffy, J. E., Folke, C., Halpern, B. S., Jackson, J. B. C., Lotze, H. K., Micheli, F., Palumbi, S. R., Sala, E., Selkoe, K. A., Stachowicz, J. J. and Watson, R.: Impacts of Biodiversity Loss on Ocean Ecosystem Services, Science, 314(5800), 787–790, doi:10.1126/science.1132294, 2006.

Yool, A., Martin, A. P., Fernández, C. and Clark, D. R.: The significance of nitrification for oceanic new production, Nature, 447(7147), 999–1002, doi:10.1038/nature05885, 2007.

Zehr, J. P. and Kudela, R. M.: Nitrogen cycle of the open ocean: from genes to ecosystems, Annual Review of Marine Science, 3(1), 197–225, doi:10.1146/annurev-marine-120709-142819, 2011.

698
699 **Figure Captions**

700 Fig.1. A schematic of the nitrogen cycling model used in this study, where microbial processes
701 include *h* as ammonium oxidation, *y* as nitrate reduction, *r* and *x* are nitrite reduction and
702 oxidation, and *u* is uptake by phototrophs. These parameters are all first order rate coefficients
703 and instantaneous fluxes are the product of the parameter and its substrate concentration.
704 Remineralization, *m*, is a fixed rate. All parameters are defined in Table 1.

705

706 Fig. 2. The ending measured concentrations (in μM) for ammonium, nitrite, and nitrate and the
707 ending seawater temperature (^{o}C), percent oxygen, and pH in all experimental tidepools used for
708 the Linear Mixed Effect model results in Table 2. The right 3 panels are rates (nmol L^{-1} h^{-1})
709 estimated from the ODE model (Eqs. 2-7), including the estimated rate of remineralization (*m*)
710 and ammonium and nitrate uptake rates in experimental tidepools. The dark horizontal line is the
711 median, the box encompasses 50% of the data and the unfilled circles are outliers. The positive
712 effect of mussels (shaded bars) on these 3 rates was greatest during the day. Linear mixed effects
713 model results are in Table 4.

714

715 Fig. 3. ODE modeled ^{15}N fits to the data for 6 representative tidepools in all four enrichment
716 experiments. The ODE model was fit individually to each tidepool, designated with unique
717 colors and symbols. Measurements are shown with symbols, while model fits at each time point
718 are designated with lines; filled symbols with solid lines are 3 separate tidepools with mussels,
719 while open symbols with dashed lines are 3 tidepools where mussels were removed. The lines
720 thus represent the differential equation model (Eqs. 2-7) fit based on the modCost function using
721 sum of squares. The symbols are the measured values (in nmol ^{15}N L^{-1}) for the corresponding

722 tidepool at each time point; note difference in axes for nitrite. Note that although tidepools
723 differed greatly in their nutrient dynamics, the model fits are generally close to the measured
724 value.
725
726 Fig. 4. The relationship between the predicted total ^{15}N (in nmol L^{-1}) (by the ODE model) and
727 observed quantity of total ^{15}N (in nmol L^{-1}) at the end of each of the $^{15}NH_4$ and $^{15}NO_3$ tracer
728 experiments. The 1:1 line is shown and indicates that the model did not, on average, lead to an
729 artificial production or loss of ^{15}N and thus provided a reasonable fit to overall ^{15}N dynamics.
730 Each estimate is per tidepool and filled symbols are night, while unfilled symbols are day.
731
732 Fig. 5. The estimated rates (nmol L^{-1} h^{-1}) of microbial nitrogen transformations based on the
733 ODE model in the left panel (Eqs. 2-7) and the source-product model (Eq. 1; e.g. Lipschultz
734 2008) with blue shading on the right. A. ammonium oxidation ($h\bar{A}$), B. nitrite oxidation ($x\overline{Ni}$), c.
735 nitrate reduction ($y\overline{Na}$), d. nitrite reduction ($r\,\overline{Ni}$). Note differences in axes; the differential
736 equation model rates are shown at 4 times the scale of the source-sink model. All other legend
737 elements as in Fig. 2.
738
739
740
741
742
743

744 Fig. 1

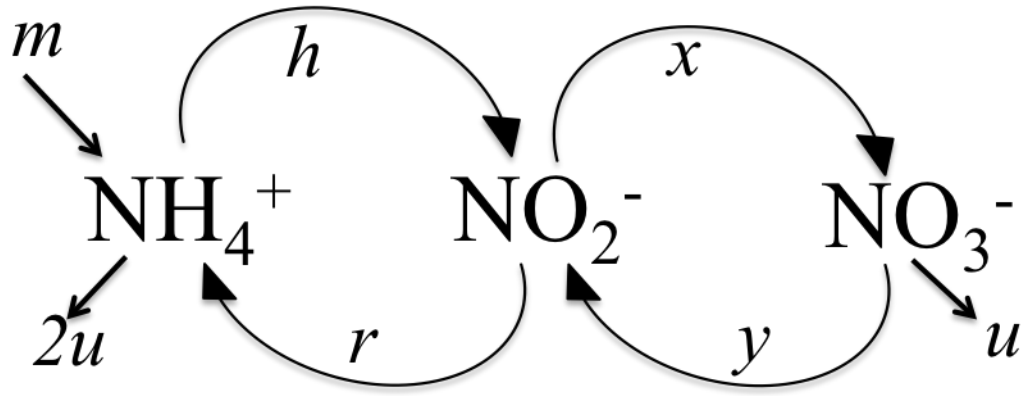

745

746

747 Fig. 2

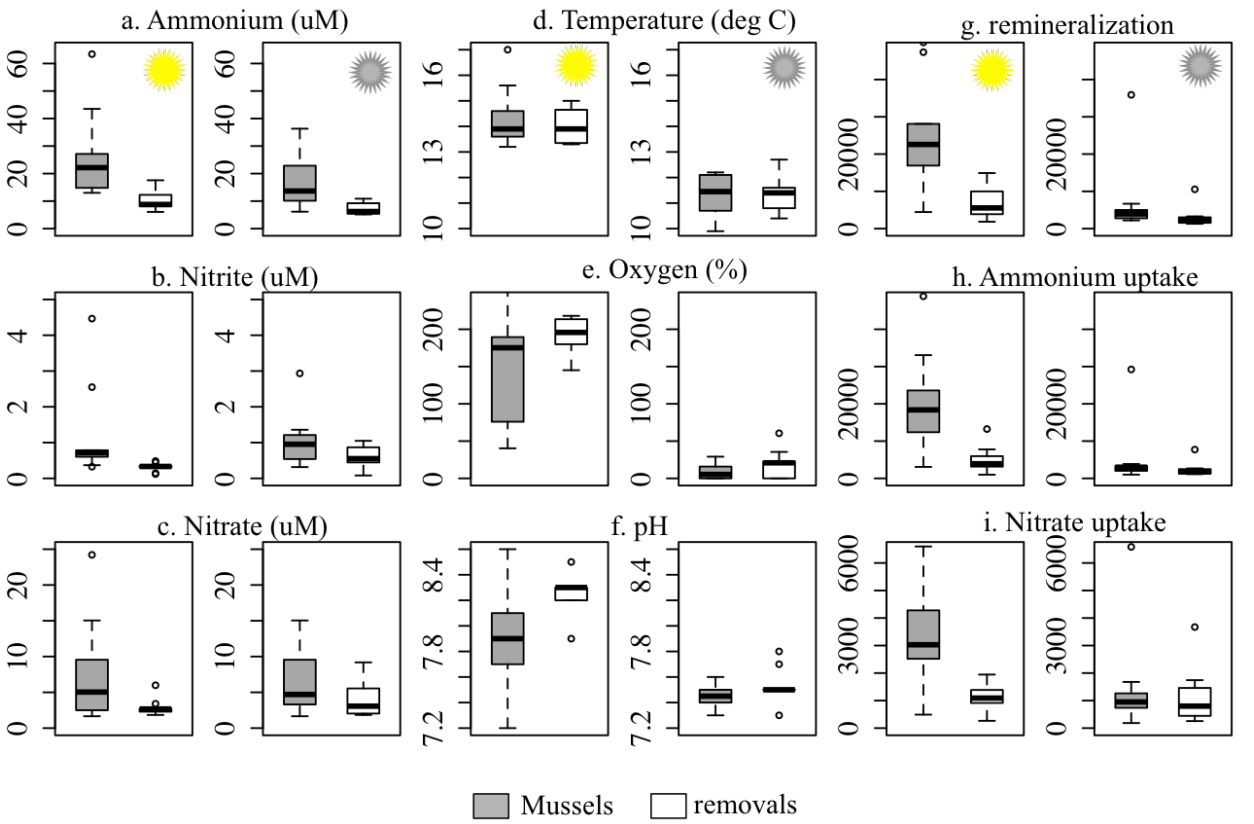

748

749

750

751

752

753

754

755

756

757

758

759

760

761 Fig. 3

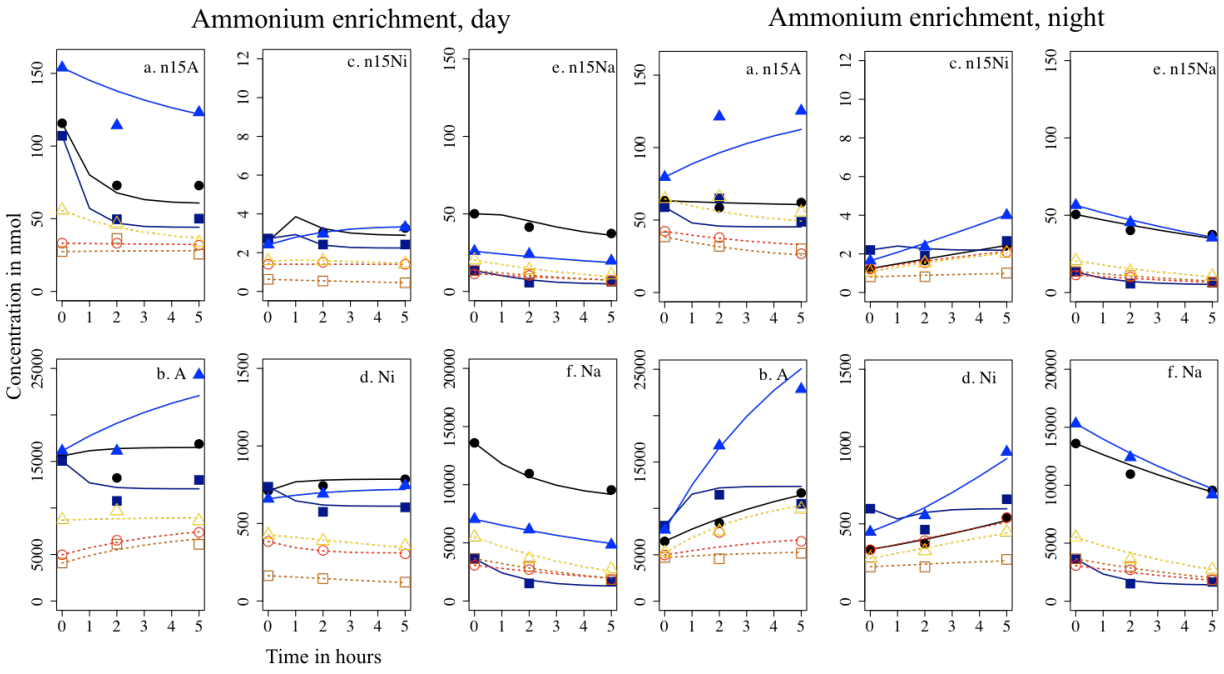

762

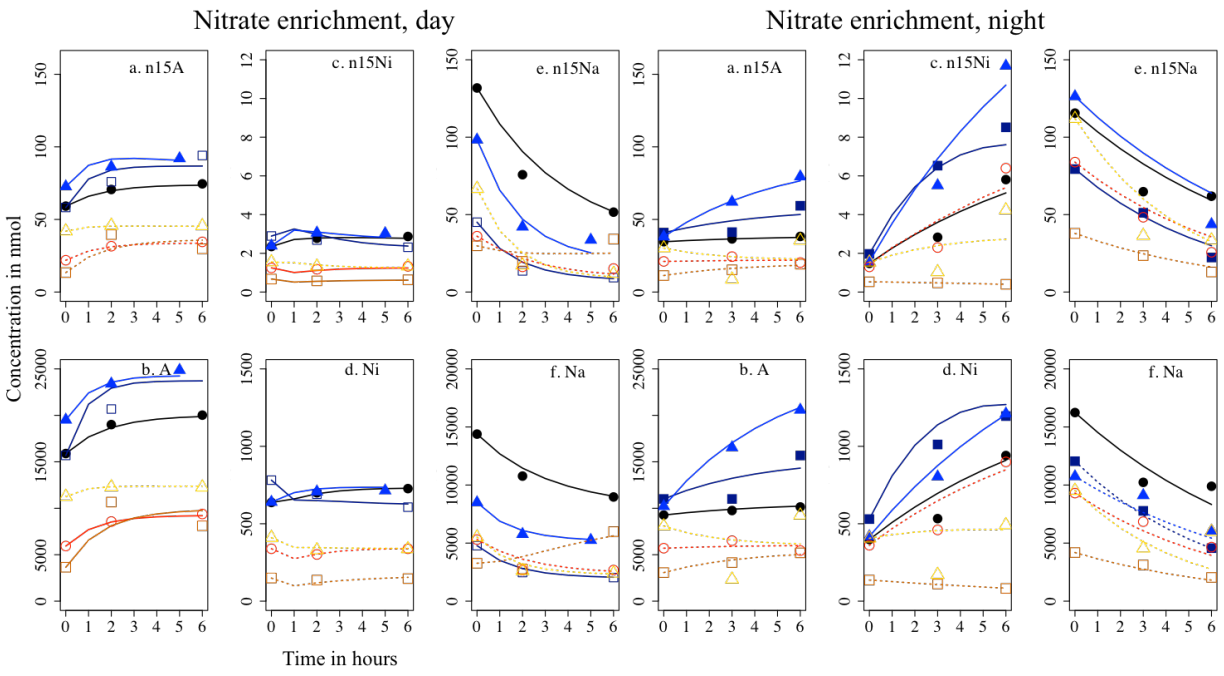

763

Fig.4

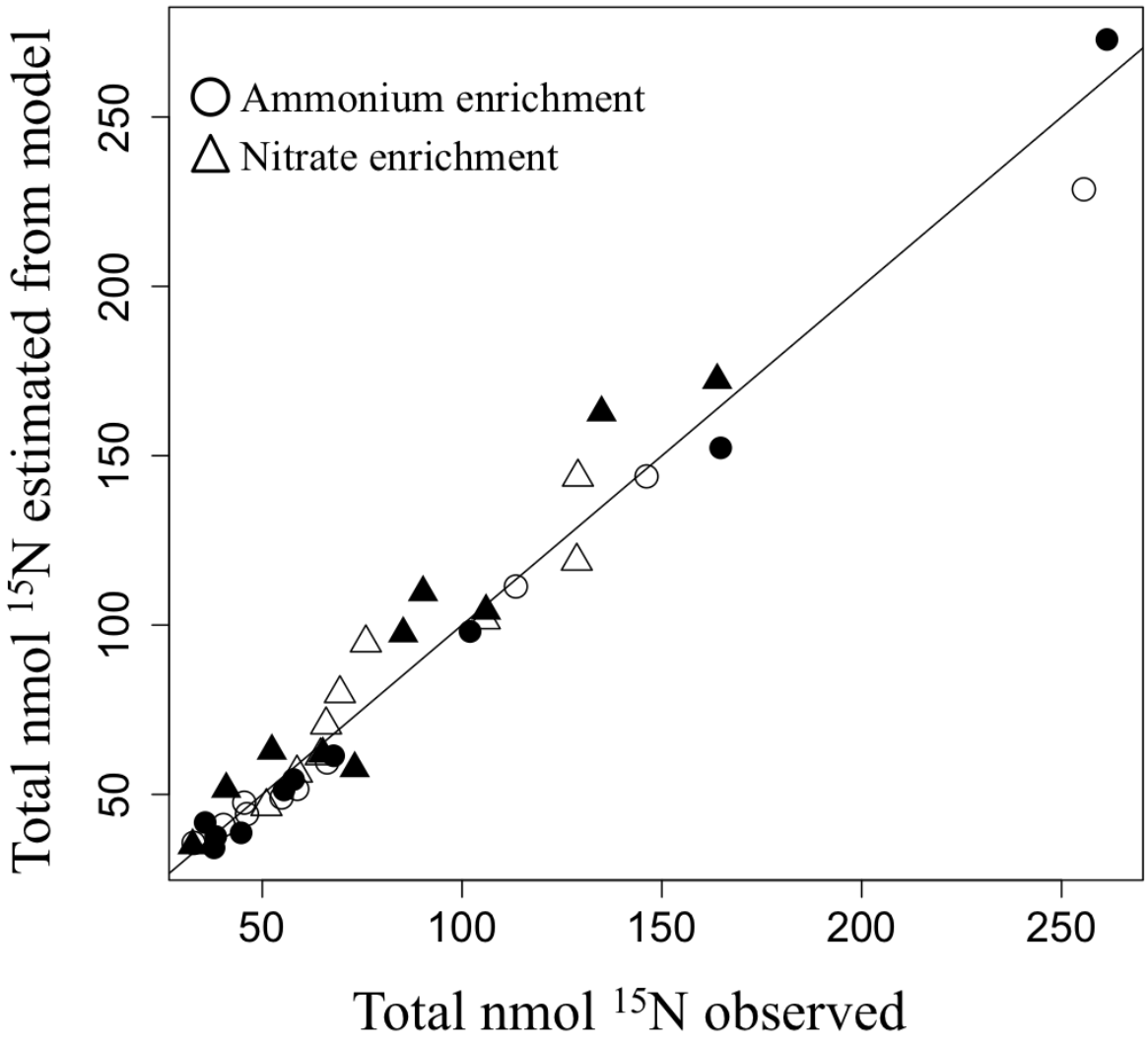
Ammonium enrichment
Nitrate enrichment
Total nmol 15N estimated from model
Total nmol 15N observed
50
100
150
200
250

Fig. 5

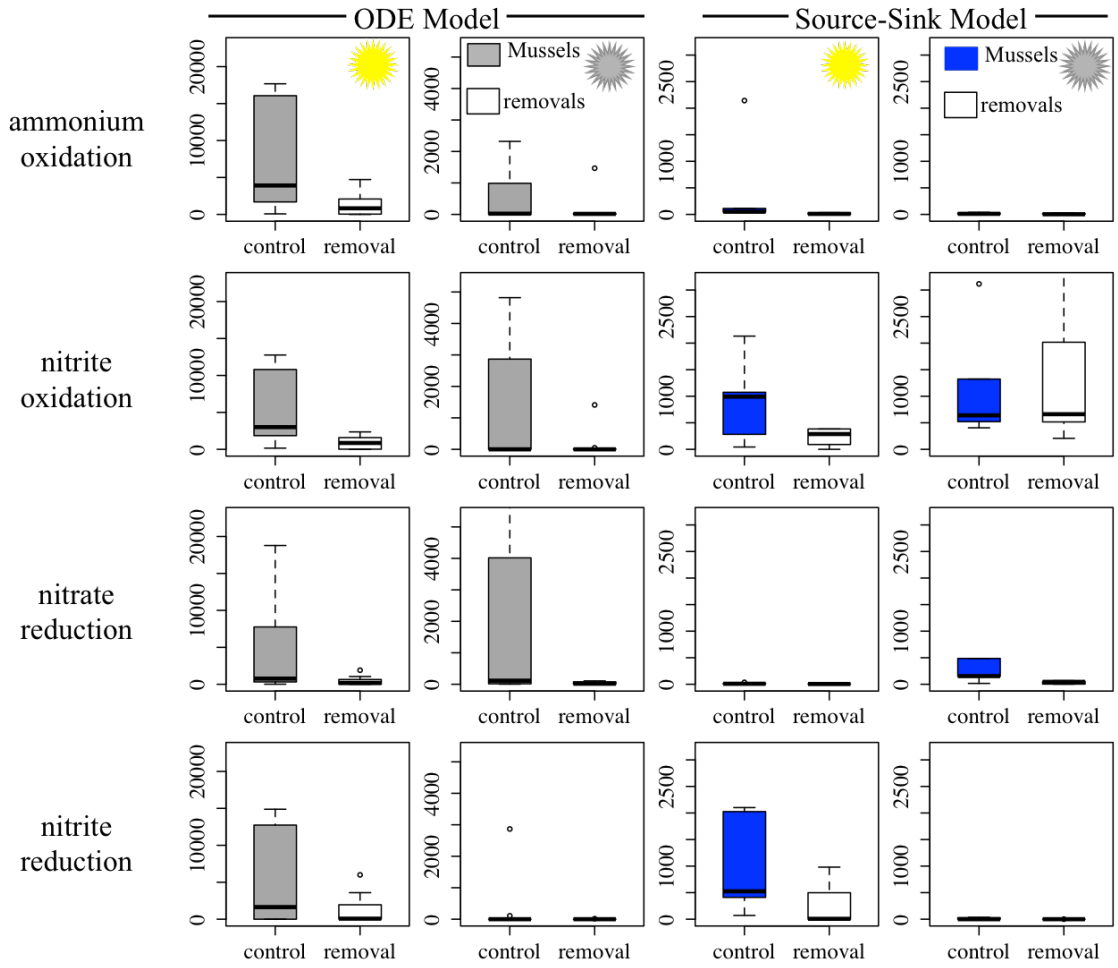
ODE Model
Source-Sink Model
Mussels
removals
ammonium oxidation
nitrite oxidation
nitrate reduction
nitrite reduction
control
removal
0
10000
20000
2000
4000
1000
2500

Table 1. A list of observed and modeled parameters used in this study.

Parameter	Definition	Method of estimation
$\delta^{15}N‰$	$[(R_{sample}- R_{atmN2})/R_{atmN2}]$ x1000, where R is $^{15}N/^{14}N$	Direct experimental measurement
A	ammonium concentration (nmol L^{-1})	Direct experimental measurement
Ni	nitrite concentration (nmol L^{-1})	Direct experimental measurement
Na	nitrate concentration (nmol L^{-1})	Direct experimental measurement
n15A	nmol L^{-1} of $^{15}NH_4$	Direct experimental measurement
n15Ni	nmol L^{-1} of $^{15}NO_2$	Direct experimental measurement
n15Na	nmol L^{-1} of $^{15}NO_3$	Direct experimental measurement
R_A	Atom % ratio of $^{15}NH_4$ or n15A/A x100	Direct experimental measurement
R_{Ni}	Atom % ratio of $^{15}NO_2$ or n15Ni/Ni x100	Direct experimental measurement
R_{Na}	Atom % ratio of $^{15}NO_3$ or n15Na/Na x100	Direct experimental measurement
m	Remineralization rate (h^{-1} L^{-1})	Estimated with ODE model
u	Uptake rate coefficient (h^{-1})	Estimated with ODE model
h	Ammonium oxidation rate coefficient (h^{-1})	Estimated with ODE model
x	Nitrite oxidation rate coefficient (h^{-1})	Estimated with ODE model
r	Nitrite reduction rate coefficient (h^{-1})	Estimated with ODE model
y	Nitrate reduction rate coefficient (h^{-1})	Estimated with ODE model

Table 2. A statistical summary of the role of mussels and day versus night on resulting seawater chemistry and temperature immediately prior to tidepool re-inundation. We used linear mixed effects models with tidepool as a random effect and log-transformed estimates for nutrient concentration; t values are given; §=0.10>p>0.05, *=p<0.05, **p<0.001. The number of observations was 40.

	Mussels	**Time of Day**	**Mussels* Time of Day**
$[NH_4^+]$	3.076*	4.225**	0.841
$[NO_2^-]$	2.421*	0.232	2.327*
$[NO_3^-]$	1.865§	0.327	1.086
Percent O_2	2.727*	6.913**	2.045§
Temperature	0.784	9.254**	0.950
pH	2.223§	3.716*	1.613

Table 3. A summary of all estimated rates by treatment in the ODE model (Eqs. 2-7). Means and (se) are shown with n=10 per treatment. The contribution of microbial transformations to overall ammonium and nitrate fluxes was quantified as the percentage that microbial activity (NH_4^+ oxidation, NO_3^- reduction, NO_2^- oxidation and reduction) contributed to all nitrogen uptake, including nitrogen uptake of phototrophs (u).

Rates (nmol L^{-1} hr^{-1})	**Mussels**		**No Mussels**	
	day	Night	day	night
Ammonium oxidation ($h\bar{A}$)	11695 (5945)	490 (262)	1435 (572)	161 (145)
Nitrite oxidation ($x\overline{Ni}$)	6980 (2433)	1904 (1173)	867 (267)	148 (140)
Nitrate reduction ($y\overline{Na}$)	4548 (2098)	2261 (1284)	435 (197)	34 (12)
Nitrite reduction ($r\,\overline{Ni}$)	9170 (5281)	298 (286)	1228 (649)	2 (2)
Remineralization (m)	25079 (4554)	7082 (3229)	6471 (1308)	3017 (868)
Ammonium uptake ($2u\bar{A}$)	20414 (4103)	5279 (2676)	4904 (1131)	2405 (618)
Nitrate uptake ($u\overline{Na}$)	3206 (530)	1465 (585)	1064 (159)	1140 (324)
% ammonium flux due to microbial activity (of total)	32 (13)	12 (10)	22 (9)	3 (2)
% nitrate flux due to microbial activity (of total)	61 (9)	30 (18)	39 (14)	8 (4)

Table 4. A statistical summary of the role of mussels, day versus night, and their interaction on the rates of nitrogen transformations (in nmol L^{-1} hr^{-1}) estimated in both our ODE models and the traditional source-product models. Linear mixed effects models using tidepool as a random effect were used on log-transformed or square-root transformed estimates from Eq. 2-7; t values are given; §=0.10>p>0.05, *=p<0.05, **p<0.001. The correlation between coefficients estimated from each method is shown in the last column; no coefficients were significant. There were 40 observations for the ODE model and 20 for the source-sink model.

	ODE Model Estimates			**Source-Product Model**			**Corr**
Rate	Mussels	Time of Day	Mussels x Time of Day	Mussels	Time of Day	Mussels x Time of Day	
Ammonium oxidation ($h\bar{A}$)	3.131*	4.168**	2.025*	2.568*	1.970§	2.080§	0.004
Nitrite oxidation ($x\overline{Ni}$)	2.709*	5.054**	2.232*	1.278	0.364	0.935	-0.216
Nitrate reduction ($y\overline{Na}$)	2.725*	1.205	0.774	0.761	4.103*	1.657	-0.021
Nitrite reduction ($r\,\overline{Ni}$)	2.032§	2.907*	1.209	2.561*	3.365*	1.172	-0.010
Remineralization (m)	4.139*	5.676**	2.722*				
Ammonium uptake ($2u\bar{A}$)	4.183*	5.478**	2.853*				
Nitrate uptake ($u\overline{Na}$)	3.336*	3.323 *	2.307 *				

Appendix A1. Example dynamics of stable nitrogen isotopes ($\delta^{15}N$) of tidepool ammonium, nitrite and nitrate for 4 separate ^{15}N enrichment experiments made at different times in a single control tidepool (with mussels). We measured values prior to the addition of tracer (T_o), followed by an immediate post-tracer measurement (T_1), and an approximately 2-3 hour (T_2) and a 5-6 hour (T_3) post-tracer measurement. The left 2 panels show the addition of enriched ammonium and the resultant nitrate and nitrite enrichment, while the right 2 panels show the addition of enriched nitrate and the resultant enrichment in ammonium and nitrite. In all cases, the $\delta^{15}N$ (‰) axis scale for the enriched source is double that of the product quantities.

Appendix A2. We show the fit of models (colored lines) to data (points) where we varied the ratio of *u* for ammonium uptake versus nitrate uptake for a single tidepool during a daytime, ammonium enrichment. This representative scenario shows that a 2:1 ratio, where phototrophic ammonium uptake is twice that of nitrate uptake, was the best fitting model. Greater or lesser ratios did not fit the data as well. Other figure attributes as in Fig 3.

Appendix A1

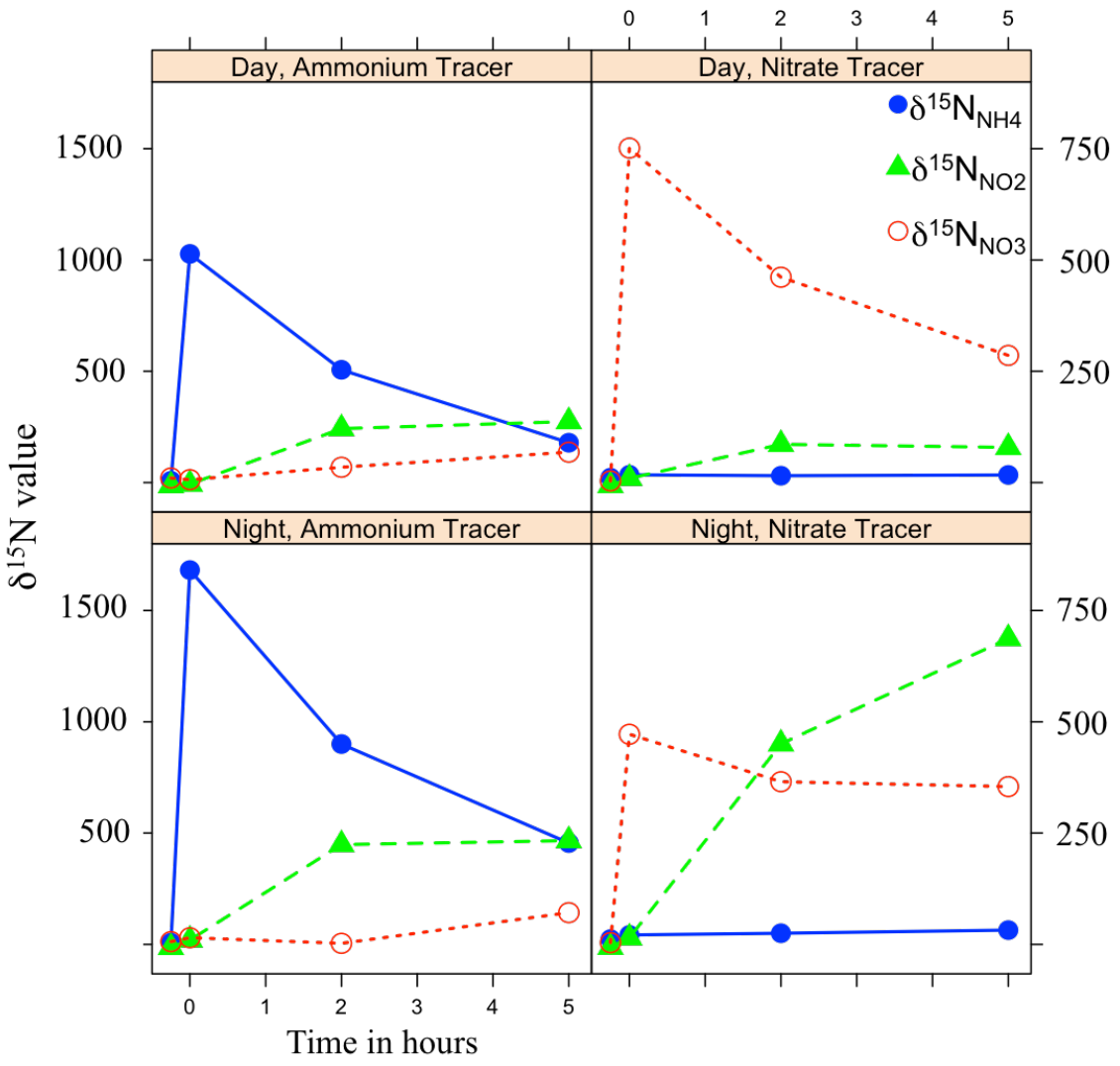
Day, Ammonium Tracer
Day, Nitrate Tracer
Night, Ammonium Tracer
Night, Nitrate Tracer
δ15NNH4
δ15NNO2
δ15NNO3
δ15N value
Time in hours
0
1
2
3
4
5
500
1000
1500
250
750

Appendix A2

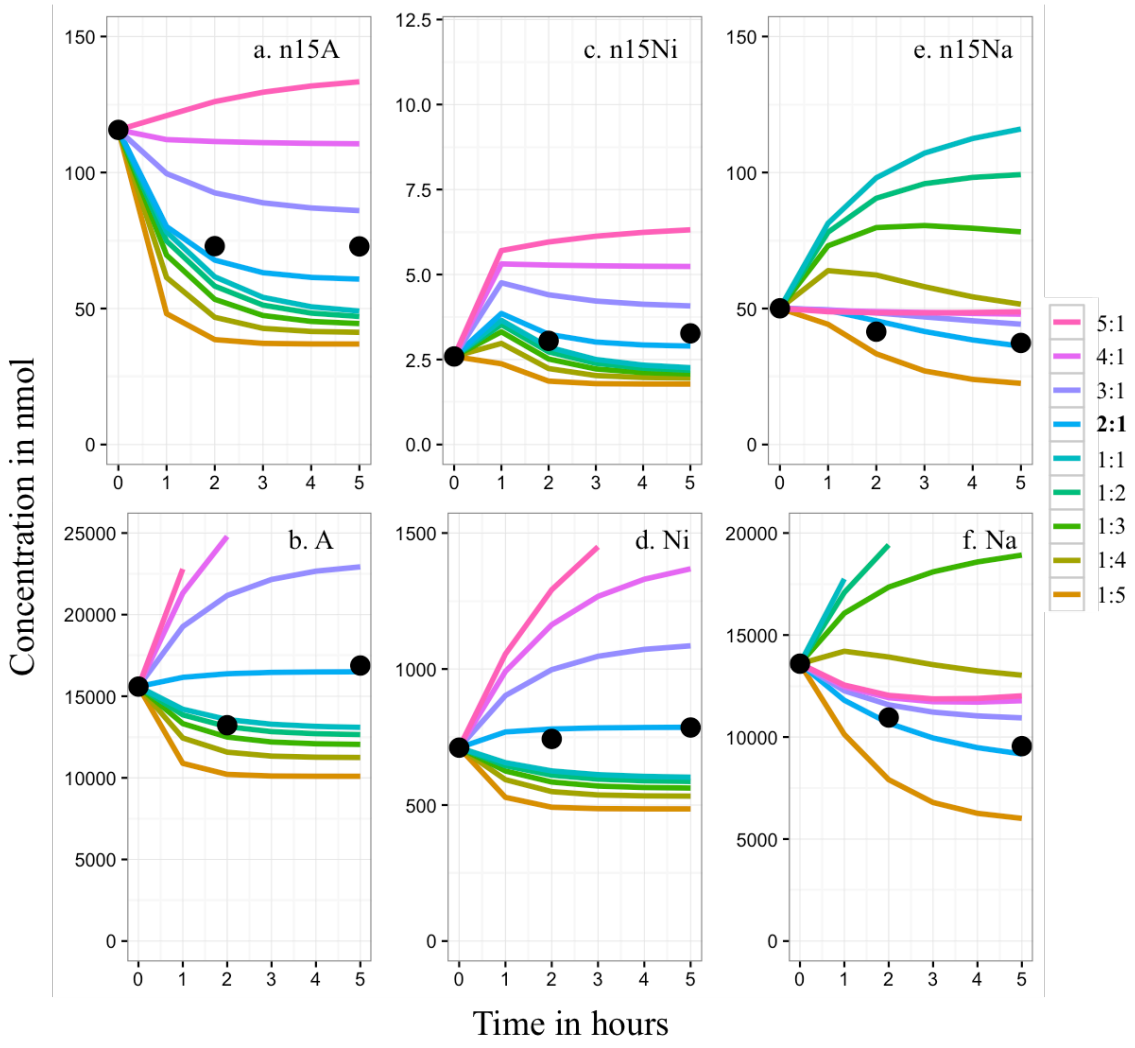
a. n15A
c. n15Ni
e. n15Na
b. A
d. Ni
f. Na
Concentration in nmol
Time in hours
5:1
4:1
3:1
2:1
1:1
1:2
1:3
1:4
1:5